Complex Permittivity of Gadolinium Gallium Garnet from 8.2 to 12.4 GHz

David A. Connelly, Hadrian Renaldo O. Aquino, Maxwell Robbins, Gary H. Bernstein, Alexei Orlov, Wolfgang Porod, Jonathan Chisum

Department of Electrical Engineering, University of Notre Dame, Indiana 46556, USA

This paper reports the measured complex permittivity of gadolinium gallium garnet from 8.2-12.4 GHz using a transmission/reflection method in a rectangular waveguide. A modification of the Nicolson-Ross-Weir method, valid for non-magnetic materials, yields an average relative dielectric constant of 11.99 and loss tangent of 5.2×10^{-3} across the band. The measured relative dielectric constant agrees well with near-DC and THz measurements. A statistical error analysis quantifying systematic and non-systematic errors indicates a standard deviation of 0.77 % and 17 % for the relative dielectric constant and loss tangent, respectively. The measured loss tangent of GGG indicates that microwave spin-wave transducers operating in the magnetostatic regime (wavelength larger than 100 μ m at 1 GHz and larger than 10 μ m at 10 GHz) will need to consider dielectric losses in addition to ohmic losses, while transducers operating near and in the exchange regime will be dominated by ohmic loss. If on-chip matching networks are required, it is recommended to use a low-order network and as thin a GGG substrate as possible to reduce the power dissipated in the network.

Index Terms—Microwave Magnetics, Microwave materials, Spin electronics, Magnetic and spintronic materials

I. INTRODUCTION

ADOLINIUM gallium garnet (GGG) is the ideal substrate for growing high-quality yttrium iron garnet (YIG) films, the magnetic material of choice for microwave magnetic circuits, due to the near-identical lattice match between GGG and YIG [1]. GGG facilitates the growth of very low loss YIG films [2], even at nanometer thicknesses, which are necessary for applications in Boolean spintronics [3], wave-based computing [4], [5], and on-chip microwave spin-wave components [6], [7]. These applications require efficient transducers to convert electromagnetic waves to spin waves [8], [9], and as a consequence, low-loss substrates at microwave frequencies.

Some uncertainty exists regarding GGG's permittivity due to conflicting reports between vendor specifications and published literature. Most GGG vendors of $\langle 111 \rangle$ GGG grown by the Czochralsky method specify a relative dielectric constant, ϵ_r , of 30 and a loss tangent, $\tan \delta$, of either 0.15 or 0.3×10^{-3} at 10 GHz [10]–[14], sometimes also specified at 77 K. However, one vendor [15] and several published measurements report that the relative dielectric constant is actually very close to 12. In [16], a substitution capacitive method (SCM) yielded $\epsilon_r = 12.11$ at 1 KHz. In [17], $\epsilon_r = 12.08$ and $\tan \delta \approx 0.02 \times 10^{-3}$ were reported with a capacitive method (CM) at 10 MHz. Time-domain spectroscopy (TDS) from 0.3-1 THz [18] resulted in a similar dielectric constant of 11.97 but a much higher loss tangent of 36×10^{-3} .

The real part of GGG's permittivity is expected to be nearly constant at microwave frequencies since optical phonon modes begin above 2.5 THz [19], [20]. Moreover, the predicted DC permittivity is $\epsilon_0 = 13.17$ as calculated with

Manuscript received XXXXX, 2021; revised XXXXX.

The authors are with the Department of Electrical Engineering, University of Notre Dame, Notre Dame, IN, 46556 USA. This work was supported by the National Science Foundation (NSF) through the Spectrum Efficiency, Energy Efficiency, and Security (SpecEES) program. Corresponding author: J. Chisum (email: jchisum@nd.edu).

the Lydanne–Sachs–Teller relation using experimentally-fitted values for the permittivity at infinity, ϵ_{∞} , and measured optical phonon modes [20]. Therefore, a dielectric constant of 12 at microwave frequencies is likely closer to the true value instead of a value of 30, referenced above. On the other hand, the loss tangent of GGG near room temperature and microwave frequencies is uncertain, yet it is clearly not constant between 10 MHz to 1 THz. In fact, the loss tangent is quite poor from 0.3 to 1 THz, most likely heavily influenced by optical phonon resonances starting above 2.5 THz.

Therefore, the goal of this investigation is to measure the complex permittivity of $\langle 111 \rangle$ oriented GGG in the microwave band to determine the suitability of GGG as a microwave substrate and, if found acceptable, to enable more complete modeling and design of efficient, integrated microwave-magnetic circuits. Here, we report measurements of the complex permittivity of GGG, measured from 8.2 to 12.4 GHz (X-band) using a transmission/reflection (TR) method [21]–[23] of a sample placed in a rectangular waveguide. Section II outlines the measurement method and setup, section III presents the results and error analysis, and section IV concludes with practical recommendations.

II. MEASUREMENT METHOD AND SETUP

A TR method using rectangular waveguides, based on Nicolson-Ross-Weir (NRW) [21], [22], is employed here to characterize the complex permittivity of GGG: a sample is inserted into a section of a waveguide and characterized using scattering parameters. Waveguide TR methods are often desirable because they provide material properties across a broad range of frequencies, in contrast to resonant methods, which provide information only at discrete frequencies [24]. However, resonant methods typically have a higher sensitivity to loss for the same amount of sample material, so they are preferred when characterizing low-loss materials. To increase

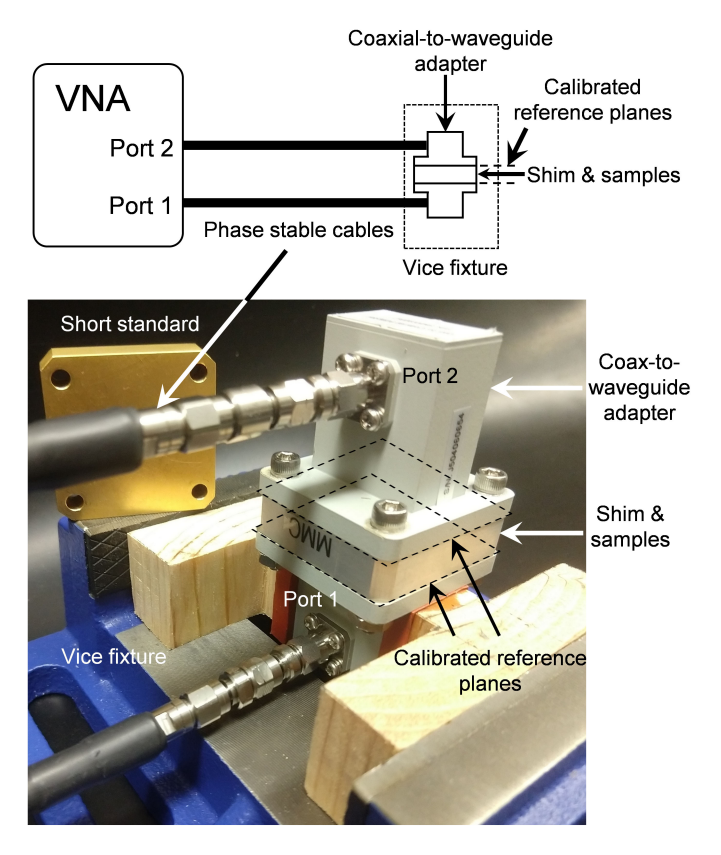


Fig. 1. TR measurement setup. Coax-to-waveguide adapters connect the shim and samples to a VNA through phase-stable cables. The calibrated reference plane is indicated by the black dashed lines at the adapter-shim interface.

sensitivity to loss while obtaining a broadband response of GGG's permittivity, we utilize a more precise NRW method, cascade multiple samples, and pay special attention to phase and mechanical repeatability, as discussed below. The specific NRW method utilized here [23], referred to as Precision NRW, is suitable for dielectrics only since it enforces that the permeability be 1 + j0, which is a valid assumption for GGG given that no static magnetic field is utilized here to induce paramagnetic behavior [18]. Thus, any measurement error will appear only in the extracted dielectric properties, not as any extracted magnetic properties. This method greatly diminishes the solution divergence of low-loss samples at frequencies when the sample thickness is an integer-multiple of a half-wavelength. Furthermore, this method also removes the need to know precisely the placement of the sample in the waveguide, thereby reducing error due to improper translation of the calibration reference planes to the sample plane.

A commercially available, single-side polished, 0.5 mm thick, $\langle 111 \rangle$ oriented GGG wafer, grown by the Czochralsky method, is obtained from MTI Corporation and diced into pieces that fit inside a WR-90 waveguide $(10.16 \times 22.86 \ \text{mm}^2).$ Additionally, a double-side polished, 0.5 mm thick, 99.9% purity alumina with a density of 3.92 g/cm³ is obtained from the same vendor to serve as a reference material since alumina is a well-characterized material. Since alumina has a similar relative dielectric constant as reported in the literature for GGG, so we expect similar challenges in phase stability

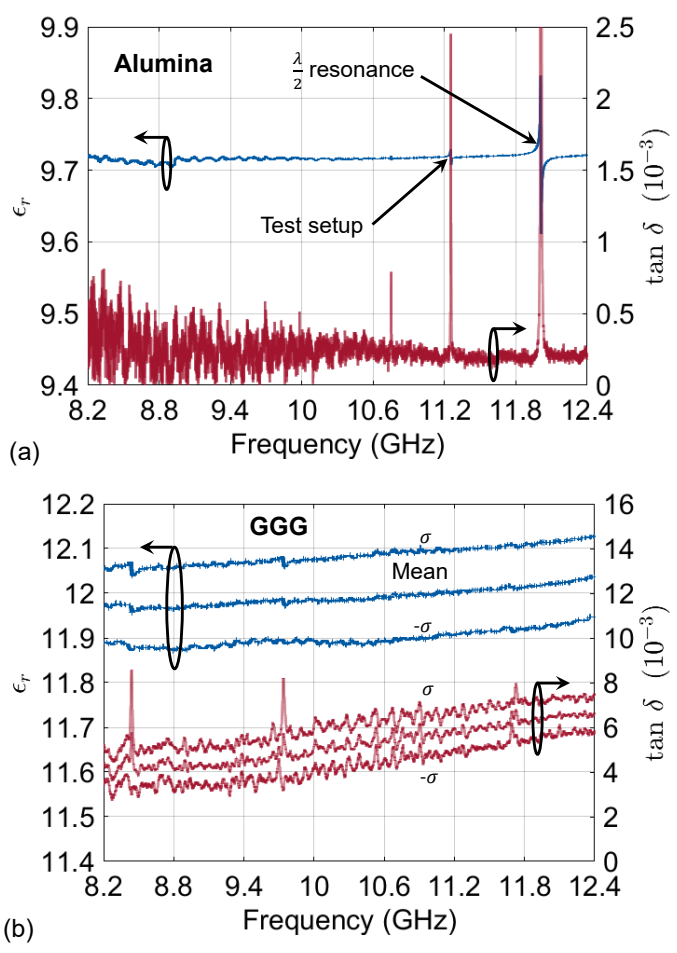


Fig. 2. Measured complex permittivity of alumina and GGG. (a) Dielectric constant and loss tangent of 99.9 % alumina. The average dielectric constant and loss tangent over frequency is 9.72 and 0.27×10^{-3} , respectively. (b) Average and standard deviation of the dielectric constant and loss tangent of GGG computed across twenty-one measurements at each frequency.

and calibration. Lastly, characterizing alumina's very low loss tangent ensures we have sufficient signal-to-noise ratio (SNR) to measure GGG's loss tangent, which is expected to be significantly higher. The vendor-supplied permittivity for the alumina sample is $\epsilon_r=9.8$ and $\tan\delta<0.1\times10^{-3}$ at 1 MHz. Eight alumina pieces and four GGG pieces are stacked and inserted into the waveguide shim for measurement; more alumina samples were utilized to increase the measurement's SNR to extract alumina's lower loss tangent.

Scattering parameters from 8.2 to 12.4 GHz in 1 MHz steps are measured using a vector network analyzer (VNA) (Keysight PNA N5225A). A thru-reflect-line (TRL) calibration [25] is performed to remove systematic errors in the measurement setup, bringing the calibration reference plane to the flange/shim interface (Fig. 1). A 50 Hz IF bandwidth is chosen for calibration to maintain very low thermal noise at each frequency. The port power was 10 dBm, the highest power capable by the PNA across X-band, to obtain a high SNR.

Because phase errors can contribute significantly to loss tangent errors [26], phase-stable cables (Gore 0Z) are connected between the VNA and the coax-to-waveguide adapters and

maintained in a nearly-fixed position throughout calibration and measurement. A seen in Fig. 1, the adapter connected to port 1 of the VNA remains secured in a vice, while the adapter connected to port 2 is moved just enough to perform the calibration steps and load samples. Any accrued phase errors due to this movement is quantified by a statistical error study explained further in section III. Alignment pins are utilized during connections of the waveguide flanges to each other, the shim, and the short in order to increase mating repeatability and minimize reflections incurred from mating mismatches.

Since multiple samples were loaded in the waveguide shim, it was important to minimize air-gaps between samples and maintain planarity. First, each sample was carefully diced to < 1 mil smaller than the waveguide cross-section. The corners of the first sample were polished to ensure a tight fit and the sample was loaded into the shim and pressed down to the surface of a temporary standoff. The corners of subsequent samples were polished to ensure a slip fit and were gently tapped onto the first sample. Finally the standoff was removed from the bottom of the shim. We note that the Precision NRW method is robust to air gaps along the axis of the waveguide and able to deembed measured air gaps in the cross-section.

III. RESULTS AND ERROR ANALYSIS

The measured relative dielectric constant and loss tangent of alumina are shown in Fig. 2(a). The real part of the permittivity averaged over frequency is 9.72, which is a 0.85 % deviation from the vendor specification of 9.8. When compared to a comprehensive study of alumina samples with various purities and densities [27] (summarized in Table I), a permittivity of 9.8 is a reasonable value given the density of this sample $(3.92 \, \text{g/cm}^3)$. For high purity alumina, the density, not minor variations in purity, determines ϵ_r .

To extract alumina's loss tangent, a flat line was fit to the upper frequency portion (11.2 to 12.4 GHz, excluding the resonances at 11.25 and 12 GHz) of the measured band, since dielectric loss is proportional to frequency and will result in a higher SNR, which is clearly observed in Fig. 2(a). The extracted loss tangent from this fit is (0.201×10^{-3}) , but this value cannot be compared in a meaningful way to the vendor's 1 MHz specification since impurities are expected to result in non-monotonic loss from 1 MHz to 10 GHz [27]. Instead, a comparison is made again to alumina samples reported in [27] at 15 GHz. The percent error of the loss tangent in [27] is less than 10% down to 1×10^{-5} . The loss tangent presented here agrees quite well and is of the same order of magnitude as the 99.9% purity grades in [27]. Given this close agreement for alumina, one can have a high degree of confidence in the measurement of GGG, which has a much higher loss tangent than alumina. It should be noted that, in general, similarity in purity grades, especially for lower grades, is not sufficient to determine alumina losses; instead, the type of purity plays a significant role [27].

A resonance corresponding to the frequency at which the sample length is equal to half a wavelength can be seen in Fig. 2(a); while Precision NRW decreases this numerical artifact, it does not entirely remove it. Another resonance,

which appears small in ϵ_r but noticeable in the loss tangent, is attributed to remaining errors in measurement, not due to any material properties of alumina.

The same measurement setup, after validation with a known alumina sample, was used to characterize GGG. The measured relative dielectric constant and loss tangent of GGG are shown in Fig. 2(b). Twenty-one measurements were taken across three calibrations, where the flanges were disconnected and reconnected from the shim for each measurement, to quantify remaining systematic errors and random errors. The results were averaged across the twenty-one measurements at each frequency, and the standard deviation was computed for each frequency, as shown in Fig. 2(b). Then, the average across all frequencies of the mean ϵ_r and mean loss tangent was computed to be 11.99 and 5.2×10^{-3} , respectively. The average standard deviation across all frequencies was found to be 0.093 and 0.89×10^{-3} for ϵ_r and loss tangent, respectively, resulting in a percent error of 0.77 % and 17 %, respectively. The results are summarized in Table II and compared with prior work near DC and at 1 THz. The dielectric constant agrees well with the published literature, and the loss tangent is between the 10 MHz and 0.3 THz reported values, as expected.

TABLE I COMPLEX PERMITTIVITY OF ALUMINA

Frequency GHz	Density g/cm ³	Purity %	ϵ_r	$\tan \delta$ 10^{-3}
15 ^a	3.99	99.9	10.07	0.28
15	3.97	99.9	9.99	0.81
15	3.93	99.9	9.84	0.30
8.2 - 12.4 [This work]	3.92	99.9	9.72	0.20
15	3.90	99.99	9.79	0.03
15	3.84	99.5	9.63	0.16
15	3.84	99.7	9.6	3.4
15	3.82	99.5	9.56	0.97

^aAll values at 15 GHz are taken from [27]

TABLE II COMPLEX PERMITTIVITY OF GGG

Method	Freq.	ϵ_r	Dev.	$\tan \delta$ 10^{-3}	Dev.	t_s mm
SCM [16]	1 kHz	12.11	0.17	-	-	0.4-0.8
CM [17]	$10\mathrm{MHz}$	12.08	1	0.02	2	0.5
TDS [18]	0.3 - 1 THz	11.97	-	36	-	0.5
NRW [This work]	8.2-12.4 GHz	11.99	0.77	5.2	17	2.08

There appears to be a slight frequency dependence in both the relative dielectric constant and loss tangent of GGG. Since the real part of permittivity reported at 10 MHz and 300 GHz indicates a nearly constant relative dielectric constant, we do not ascribe the relative dielectric constant's frequency dependence to the material. One possible source for this frequency dependence is additional reflections, not modeled correctly by NRW, arising from tiny air gaps between the stacked samples. Despite every effort to stack samples so as to achieve a uniform overall thickness, these air gaps may arise due to sample thickness variations (on the order of a

few micrometers), thereby preventing samples from stacking perfectly flat on top of each other. A slight frequency dependence of the loss tangent might be expected given the drastic change from 10 MHz to 0.3 THz, but without knowledge of the impurities and being far from any optical-phonon resonances, it is difficult to analyze with certainty. Thus, the authors recommend the loss tangent also be taken as nearly constant over this measured band and that future measurements be done over a wider band to further characterize the frequency response.

IV. CONCLUSION

The loss tangent of GGG at X-band, while not as high as at 300 GHz, is about four times worse than state-of-the-art RF PCB laminates such as Rogers substrates (tan $\delta=1.4\times10^{-3}$). Dielectric losses for a microstrip on GGG will start being comparable to ohmic losses when the microstrip width is larger than 100 μm at 1 GHz and larger than 10 μm at 10 GHz [28]. This means that microwave spin-wave transducers operating in the magnetostatic regime will need to consider dielectric losses in GGG, while transducers operating near and in the exchange regime will be dominated by ohmic loss.

The dielectric loss of GGG plays a more crucial role when integrating matching networks on the same substrate as spin-wave transducers. Since volume-spin-wave transducers typically have much smaller impedances than the RF system $(50\,\Omega)$, requiring an aggressive impedance transformation ratio (ITR), a significant amount of power will be dissipated in the network instead of being delivered to the transducer [29]. Under these load conditions, the network's efficiency becomes increasingly sensitive to the network's ohmic or dielectric losses, which would otherwise be acceptable at a lower ITR. Therefore, it is recommended to use lower order (less complex) matching networks and the thinnest GGG substrate possible to help reduce matching network losses.

REFERENCES

- [1] M. Wu, "Nonlinear Spin Waves in Magnetic Film Feedback Rings," in *Solid State Phys.*. Elsevier, 2010, vol. 62, pp. 163–224.
- [2] J. Ding, T. Liu, H. Chang, and M. Wu, "Sputtering Growth of Low-Damping Yttrium-Iron-Garnet Thin Films," *IEEE Magn. Lett.*, vol. 11, pp. 1–5, 2020.
- [3] A. Mahmoud, F. Ciubotaru, F. Vanderveken, A. V. Chumak, S. Hamdioui, C. Adelmann, and S. Cotofana, "Introduction to spin wave computing," J. Appl. Phys., vol. 128, no. 16, p. 161101, Oct 2020.
- [4] G. Csaba, A. Papp, and W. Porod, "Perspectives of using spin waves for computing and signal processing," *Phys. Lett. A*, vol. 381, no. 17, pp. 1471–1476, may 2017. [Online]. Available: http://www.sciencedirect.com/science/article/pii/S0375960116316486
- [5] A. Papp, W. Porod, A. I. Csurgay, and G. Csaba, "Nanoscale spectrum analyzer based on spin-wave interference," Sci. Rep., vol. 7, no. 1, p. 9245, Aug. 2017. [Online]. Available: https://www.nature.com/articles/s41598-017-09485-7
- [6] Microsystems Technology Office, Broad Agency Announcement 16-36 Magnetic Miniaturized and Monolithically Integrated Components (M3IC), June 2016.
- [7] M. Geiler, S. Gillette, M. Shukla, P. Kulik, and A. I. Geiler, "Microwave Magnetics and Considerations for Systems Design," *IEEE J. Microw.*, vol. 1, no. 1, pp. 438–446, 2021.
- [8] D. A. Connelly, G. Csaba, H. R. O. Aquino, G. H. Bernstein, A. Orlov, W. Porod, and J. Chisum, "Efficient electromagnetic transducers for spin-wave devices," *Sci. Rep.*, vol. 11, no. 1, p. 18378, Dec. 2021. [Online]. Available: https://doi.org/10.1038/s41598-021-97627-3

- [9] H. R. O. Aquino, D. Connelly, A. Orlov, J. Chisum, G. H. Bernstein, and W. Porod, "Design of a Coplanar-Waveguide-Based Microwave-to-Spin-Wave Transducer," *IEEE Trans. Magn.*, pp. 1–1, 2021.
- Spin-Wave Transducer," *IEEE Trans. Magn.*, pp. 1–1, 2021.

 [10] P. S. Corporation, "Gadolinium Gallium Garnet," Aug. 2021.

 [Online]. Available: https://princetonscientific.com/materials/substrates-wafers/gadolinium-gallium-garnet/
- [11] Crystal Datasheet Substrates: Gadolinium Gallium Garnet, Crystal, Aug. 2021. [Online].

 Available: https://crystal-gmbh.com/shared/downloads/datenblaetter/substrates_de/GGG_Gadolinium_Gallium_Garnet.pdf
- [12] Gallium Gadolinium Garnet (Gd₃Ga₅O₁₂ or GGG) single crystal, Del Mar Photonics, Aug. 2021. [Online]. Available: http://www.dmphotonics.com/GGG_crystal/Gallium%20Gadolinium% 20Garnet%20(Gd3Ga5O12%C2%A0or%20GGG)%20substrate% 20material%20for%20magneto%20%E2%80%93%20optical% 20films%20and%20high%20T%20superconductors.htm
- [13] Gadolinium Gallium Garnet (GGG]), Alineason Materials and Technology, Aug. 2021. [Online]. Available: https://www.alineason.com/en/produkt/gadolinium-gallium-garnet-ggg/
- [14] Gallium Gadolinium Garnet (GGG), SufaceNet, Aug. 2021.
 [Online]. Available: https://www.surfacenet.de/gallium-gadolinium-garnet-ggg.html
- [15] Single Crystalline Substrates MgO, ZnO, GGG, GSGG, Molecular Technology GmbH, Aug. 2021. [Online]. Available: http://www.mt-berlin.com/frames_cryst/descriptions/substrates.htm
- [16] K. Lal and H. K. Jhans, "The dielectric constant of gadolinium gallium garnet and α-Al₂O₃ single crystals," *J. Phys. C: Solid State Phys.*, vol. 10, no. 8, pp. 1315–1319, Apr. 1977.
- [17] K. K. Kumar, G. Sathaiah, and L. Sirdeshmukh, "Dielectric Properties and Electrical Conductivity Studies on Gd3Ga5O12 Single Crystals," *Int. J. Chem. Sci.*, vol. 9, no. 1, pp. 239–244, Mar. 2011.
- [18] M. Sabbaghi, G. W. Hanson, M. Weinert, F. Shi, and C. Cen, "Terahertz response of gadolinium gallium garnet (GGG) and gadolinium scandium gallium garnet (SGGG)," *J. Appl. Phys.*, vol. 127, no. 2, p. 025104, Jan. 2020.
- [19] K. Ghimire, H. F. Haneef, R. W. Collins, and N. J. Podraza, "Optical properties of single-crystal Gd₃Ga₅O₁₂ from the infrared to ultraviolet," *Phys. Status Solidi B*, vol. 252, no. 10, pp. 2191–2198, 2015.
- [20] K. Papagelis, J. Arvanitidis, E. Vinga, D. Christofilos, G. A. Kourouklis, H. Kimura, and S. Ves, "Vibrational properties of (Gd_{1-x}Y_x)₃Ga₅O₁₂ solid solutions," *J. Appl. Phys.*, vol. 107, no. 11, p. 113504, Jun. 2010. [Online]. Available: http://aip.scitation.org/doi/full/10.1063/1.3393259
- [21] A. M. Nicolson and G. F. Ross, "Measurement of the Intrinsic Properties of Materials by Time-Domain Techniques," *IEEE Trans. Instrum. Meas.*, vol. 19, no. 4, pp. 377–382, Nov. 1970.
- [22] W. Weir, "Automatic measurement of complex dielectric constant and permeability at microwave frequencies," *Proc. IEEE*, vol. 62, no. 1, pp. 33–36, jan 1974.
- [23] J. Baker-Jarvis, E. Vanzura, and W. Kissick, "Improved technique for determining complex permittivity with the transmission/reflection method," *IEEE Trans. Microw. Theory Tech.*, vol. 38, no. 8, Aug. 1990.
- [24] J. Baker-Jarvis, M. D. Janezic, and D. C. Degroot, "High-frequency dielectric measurements," *IEEE Instrum. Meas. Mag.*, vol. 13, no. 2, pp. 24–31, Apr. 2010.
- [25] G. Engen and C. Hoer, "Thru-Reflect-Line: An Improved Technique for Calibrating the Dual Six-Port Automatic Network Analyzer," *IEEE Trans. Microw. Theory Tech.*, vol. 27, no. 12, pp. 987–993, Dec. 1979.
- [26] P. Galvin, "Investigation of Magnitude and Phase Errors in Waveguide Samples for the Nicolson-Ross-Weir Permittivity Technique," Master's thesis, University of New Hampshire, U.S.A, 2016.
- [27] R. Vila, M. González, J. Mollá, and A. Ibarra, "Dielectric spectroscopy of alumina ceramics over a wide frequency range," *J. Nucl. Mater.*, vol. 253, no. 1-3, pp. 141–148, Mar. 1998.
- [28] D. M. Pozar, Microwave Engineering, 4th ed. Singapore: John Wiley and Sons, Inc., 2012.
- [29] A. M. Niknejad, Electromagnetics For High-Speed Analog and Digital Communication Circuits, 2nd ed. New York, NY, U.S.A.: Cambridge University Press, 2007.